Full-body postural alignment analysis through barycentremetry.

Marc Khalifé, MD, PhD [1,2,3,*], Claudio Vergari, PhD [3], Ayman Assi, PhD [3,4], Pierre Guigui, MD, PhD [1,2], Valérie Attali, MD, PhD [3,5,6], Rémi Valentin [3,5,6], Saman Vafadar, PhD [3], Emmanuelle Ferrero, MD, PhD [1,2], Wafa Skalli, PhD [3]

[1] Orthopaedic Surgery Department, Spine Unit, Hôpital Européen Georges Pompidou, 20 rue Leblanc, 75015 Paris, France.

[2] Université Paris-Cité, Paris, France.

[3] Arts et Métiers Institute of Technology, Université Sorbonne Paris Nord, IBHGC - Institut de Biomécanique Humaine Georges Charpak, HESAM Université, 75013 Paris, France.

[4] Faculty of Medicine, Saint-Joseph University, Beirut, Lebanon.

[5] Service des Pathologies du Sommeil (Département "R3S"), Hôpitaux Universitaires Pitié Salpêtrière – Charles Foix, Assistance Publique Hôpitaux de Paris (APHP), Paris, France

[6] UMRS1158 Neurophysiologie Respiratoire Expérimentale et Clinique, Sorbonne Université, INSERM, Paris, France

** Corresponding author: Dr Marc KHALIFÉ. marc.khalife@aphp.fr*

20 rue Leblanc, 75015 Paris, France.

ORCID ID: 0000-0001-9022-3336. Tel: +33(0)1.56.09.20.00

ACKNOWLEDGMENT

The authors thank the SOFCOT (French Society for orthopedic surgery) for the research grant allocated to Marc Khalifé.

There are no conflicts of interest relative to the present study to disclose.

ETHICS

This study was approved by regional ethics committee (approval N° 6001 and N°6061, C.P.P. Ile-de France VI).

Keywords: alignment, center of mass, barycentre, barycentremetry, posture, full-body, compensation mechanism, lordosis, kyphosis, big belly, ODHA, pelvic tilt

ABSTRACT

Study design: Multicentric retrospective

Objective: The study of center of mass (COM) locations (i.e. barycentremetry) can help us understand postural alignment. This study goal was to determine relationships between COM locations and global postural alignment X-ray parameters in healthy subjects. The second objective was to determine the impact on spinopelvic alignment of increased distance between anterior body envelope and spine at lumbar apex level.

Summary of background data: Unexplored relationship between COM location and spinopelvic parameters.

Methods: This study included healthy volunteers with full-body biplanar radiograph including body envelope reconstruction, allowing the estimation of COM location. The following parameters were analyzed: lumbar lordosis (LL), thoracic kyphosis (TK), cervical lordosis (CL), pelvic tilt (PT), Sacro-femoral angle (SFA), Knee flexion angle (KFA), sagittal odontoid-hip axis angle (ODHA). The following COM in the sagittal plane were located: whole body, at thoracolumbar inflexion point, and body segment above TK apex. The body envelope reconstruction also provided the distance between anterior skin and the LL apex vertebral body center ("SV-L distance").

Results: This study included 124 volunteers, with a mean age of 44±19.3. Multivariate analysis confirmed posterior translation of COM above TK apex with increasing LL (*p=0.002*) through its proximal component, and posterior shift of COM at inflexion point with increasing TK (*p=0.008*). Increased SV-L distance was associated with greater ODHA (r=0.4) and more anterior body COM (r=0.8), caused by increased TK (r=0.2) and decreased proximal and distal LL (both r=0.3), resulting in an augmentation in SFA (r=0.3) (all $p<0.01$).

Conclusions: Barycentremetry showed that greater LL was associated with posterior shift of COM above thoracic apex while greater TK was correlated with more posterior COM at inflexion point. Whole-body COM was strongly correlated with ODHA. This study also exhibited significant alignment disruption associated with increased abdominal volume, with compensatory hip extension.

Level of evidence: II

Key points

1. Increased lumbar lordosis is associated with more posterior center of mass location of body segment above thoracic kyphosis apex, through its proximal component.

2. Increased thoracic kyphosis is associated with more posterior center of mass location at thoraco-lumbar inflexion point.

3. Odontoid-hip axis (ODHA) is strongly correlated with whole-body center of mass.

4. “Big belly effect”: increased abdominal distance is associated with more anterior location of whole-body center of mass and ODHA associated with increased TK and decreased LL, resulting in compensation through hip extension.

INTRODUCTION

Sagittal alignment of the spine has become a paramount parameter to take into account when treating patients with spinal degenerative and deformity conditions. It has been extensively demonstrated in literature that sagittal malalignment was correlated with poorer quality of life scores [1,2]. Hence, determining physiological curvatures of the spine appears of utmost importance. Strong relationships between lumbar lordosis and pelvic parameters have been described by Legaye et al. [3]. Pelvic parameters have also been used to describe morphological classification of the lumbar spine [4,5]. Further, variations of spinal sagittal alignment according to gender, age or race were reported in the literature [6–8]. However, even though lumbar lordosis can be estimated according to pelvic parameters, thoracic and cervical curvatures cannot be predicted based on those radiographic parameters [9]. Thus, it appears relevant to look for other parameters to determine physiological postural alignment of the body.

The center of mass is the point of application of the force of gravity resulting from the distribution of body mass. The study of center of mass locations (i.e. barycentremetry) can help us understand postural alignment. Duval-Beaupère et al. published a barycentremetric study using X-rays and a gamma ray scanner in order to determine the center of mass supported by each vertebra and the coxo-femoral joints [10]. Anterior displacement of these centers of mass increase mechanical constraints by augmenting lever arm on vertebral bodies [11]. This mechanism is associated with increased risk of fracture [11], and could explain certain mechanical complications in adult spinal deformity surgery, due to increased stress on upper instrumented vertebra. Later, Schwab and Steffen et al. studied body gravity line position using force plates [12,13]. Body gravity line reflects global alignment, and as it moves anteriorly,

the body exits cone of economy described by Dubousset and hence increases energy expenditure to maintain posture [14]. More recently, body envelope reconstruction on EOS® images has been validated to provide a reliable estimation of gravity line position, without having to use a force plate [15,16], thanks to trunk body density estimations, given by Dempster and Amabile et al. [17,18]. They allow calculation of centers of mass location for each body segment and the sum of the overlying segments.

This holistic approach of standing posture analysis allows taking into account subject's body mass and gravity loads thanks to barycentremetry, which appears essential when analyzing global posture. Indeed, it has been demonstrated that body mass index (BMI) influenced age-adjusted normative values of pelvic tilt (PT), pelvic incidence-lumbar lordosis mismatch and global alignment parameters [19]. However, the relationships between spinopelvic parameters and center of mass (COM) locations remain unclear.

The objective of this study was to determine the relationships between COM locations and global postural alignment with full-body X-ray parameters in healthy subjects. The second objective was to determine the impact of increased distance between anterior body envelope and spine at lumbar apex level on spinopelvic alignment.

METHODS

Population

This multicentric study retrospectively included healthy volunteers from previous studies, all aged above 18 years. Volunteers presented no major pain in the spine, hip or knee. Exclusion criteria were: any musculoskeletal deformity, scoliosis with a Cobb angle >15°, spondylolisthesis, history of spinal surgery, and hip or knee replacement. All participants had a full-body biplanar radiograph (EOS™ system, Alphatec, CA, USA) in free-standing position (in upright position, fingers positioned on the cheeks or clavicles, and one foot slightly

forward) [8]. This study was approved by regional ethics committee (approval N° 6001 and N°6061, C.P.P. Ile-de France VI). All participants provided their informed written consent, allowing the use of their data for the present study.

Parameters

Body envelope, spinopelvic and lower limb 3D reconstructions were performed based on biplanar radiographs by a specifically trained physician, according to previously validated semi-automated methods [20,21]. First the spinal line from C3 to L5 was drawn by the user on the frontal and lateral views. The software then generated a 3D spine reconstruction and retro-projected the 3D models of the vertebra on the radiographs. This model was then manually adjusted to precisely fit vertebral contours visible on the radiographs. Similarly, the 3D models of the pelvis and lower limbs were carried out, first by defining anatomical reference points on bone contours and then by adjusting the generated reconstruction. Last, the odontoid tip was marked.

Body envelope was then generated after having placed anatomical landmarks on the spine, crotch and joint centers. Similarly, the generated model was then manually adjusted on skin contours (**Figure 1**). The body envelope reconstruction also provided the "skin to vertebra" distance at the LL apex ("SV-L distance"), measured horizontally between anterior envelope and the center of the vertebral body (**Figure 2**). The same distances were calculated at the inflexion point ("SV-IP") and thoracic apex levels ("SV-T").

The model also includes a regionalization of the body (head, thorax, abdomen, upper and lower limbs), and each region was assigned mass densities according to Amabile et al. [17](**Figure 3**). This allowed to calculate the body COM location relative to a 3D reference originating from the center of the femoral heads' axis. Furthermore, the trunk was virtually divided into axial slices per vertebral level (**Figure 3**). COM locations of body slice at these

three following levels were analyzed: at LL apex, at TK apex and at thoracolumbar inflexion point. More global COM locations were also analyzed: the whole-body COM as well as cumulative segments above LL apex, above inflexion point and above TK apex (Figure 2).

All radiographic data were collected from 3D reconstructions:

- Global spinal alignment parameters: Sagittal vertical axis (SVA), T1 pelvic angle (TPA), spino-sacral angle (SSA), and sagittal odontoid-hip axis angle (ODHA) [22].
- Spinal parameters: Lumbar lordosis (LL) was measured from L1 upper endplate to the S1 plateau, distal LL (LLdist) from L4 upper endplate to the S1 plateau, and proximal LL (LLprox) from L1 upper endplate to L4 upper endplate.

  Thoracic kyphosis (TK) was measured from T1 upper endplate to L1 upper endplate. Proximal TK (TKprox) was defined as the angle between T1 and T5 upper endplates, middle TK (TKmid) between T5 lower ant T9 upper endplates, and distal TK (TKdist) between T9 lower and L1 upper endplates [23]. This distinction was performed to account for each segment as they may vary differently [24].

  Cervical lordosis (CL) was measured between C3 upper and T1 upper endplate, distal CL (CLdist) from C6 upper endplate to T1 upper endplate and proximal CL (LLprox) from C3 lower to C6 upper endplate. This distinction was performed to account for each segment as they may vary differently [25].
- Pelvic parameters: Standard pelvic parameters were collected: pelvic incidence (PI), PT and sacral slope (SS) [3].
- Lower limb parameters: Sacro-femoral angle (SFA), Knee flexion angle (KFA), Ankle flexion angle (AA) and Pelvic shift (PSh) [26]. These parameters result from the left and right lower limbs values mean.

Statistical analysis

First, a global description of the cohort was made, with parameters expressed by their means ± standard deviations (SD). All variables were tested for normality using Shapiro-Wilk's. By convention, lordosis is expressed by negative values as opposed to kyphosis. Correlations between barycentremetric parameters with demographic and radiographic parameters were looked for.

Multivariate analyses were then performed to confirm univariate correlations, as age and body mass index (BMI) were correlated with certain barycentremetric parameters. Six models were carried out, to explain the following variables: PT, LL, CT, CL, SFA and KFA. For each multiple linear regression, parameters presenting a correlation higher than 0.2 were included in the model.

All statistical analyses have been carried out using RStudio (version 1.2.1578), with p-values lower than 0.05 considered significant.

RESULTS

This study included 124 healthy volunteers, with a mean age of 44±19.3 years, ranging from 20 to 88. There were 58.1% of males (n=72). Body mass index ranged from 16.7 to 29.8, with a mean of 23.4±2.9 $kg.m^{-2}$. Radiographic and barycentremetric parameters values in the cohort are reported in **Table 1**. Whole-body COM was significantly correlated with BMI and age (**Table 2**). BMI was significantly correlated with age (r=0.5, $p<0.001$).

Pelvic parameters

PI presented no correlation with COM locations nor SV-L, SV-T and SV-IP distances. PT significantly increased with SV-L and SV-IP distances with respective correlations of 0.4 and 0.3 (both $p<0.001$) (**Table 3**). Pelvic retroversion was significantly correlated with more

posterior COM location at LL apex (r=-0.3, *p<0.001*). Multivariate linear regression confirmed the association between greater pelvic tilt with more posterior COM at LL apex and greater SV-L distance (**Table 4**).

Spinal curvatures

Lumbar lordosis was correlated with SV-L distance (r=0.5), SV-IP distance (r=0.2), COM above inflexion point (r=0.2) and above TK apex (r=0.4) (**Table 3**). Multivariate analysis confirmed posterior translation of COM above TK apex with increasing lumbar lordosis (*p=0.002*) (**Figure 4**, **Table 4**). When focusing on LL components, this association only remained significant with LLprox.

Thoracic kyphosis was correlated with SV-T distance (r=0.5, *p<0.001*) and COM location at inflexion point (r=-0.2, *p=0.008*) (**Table 3**). Multivariate regression ascertained posterior translation of COM at inflexion point with increasing TK (*p<0.001*) (**Figure 4**, **Table 4**). When focusing on the three components of TK, this association remained significant only for middle TK.

Cervical curvature was not associated with COM parameters but presented significant correlations with the three distance parameters (**Table 3**). SV-L distance correlated with proximal cervical lordosis (r=-0.4, *p<0.001*), whereas distal CL was independent of this distance. Multivariate analysis confirmed significant association between CL and SV-T distance (**Table 4**).

Lower limbs

SFA presented significant correlations with all COM and distance parameters (**Table 3**). Multivariate regression confirmed that higher SFA was significantly associated with more

posterior whole-body COM location (*p<0.001*) (**Table 4**). A greater KFA was significantly correlated with a more posterior location of COM body (r=-0.2, *p=0.03*).

Global alignment

ODHA and SVA presented strong correlations with all COM and distance parameters, reaching 0.9 between ODHA and COM above TK apex (*p<0.001*) (**Table 3**, **Figure 5**). Increased SV-L distance was correlated with more anterior body COM and greater ODHA (respectively r=0.8 and 0.4) as well as greater CL, TK, SFA and lower proximal and distal LL (**Table 5**). Multivariate analysis confirmed significant association between SV-L distance and COM body, ODHA, TK, SFA and both distal and proximal LL (**Table 5**). **Figure 6** illustrates spinopelvic changes significantly associated with increased SV-L distance after multivariate regression.

DISCUSSION

Barycentremetric study allows a better comprehension of spinal curvatures, global alignment and compensation mechanisms. This study demonstrated that there were significant correlations of COM and body envelope with spinopelvic and global alignment. Thus, a greater lumbar lordosis was associated with a more posterior location of COM above TK apex, and larger TK was associated with a posterior translation of COM at inflexion point. ODHA was strongly correlated with whole-body COM location, and other segmental COM. Last, the "big belly effect" associated a more anterior body COM and ODHA with decreased proximal and distal LL, increased TK, resulting in compensating increased SFA.

Barycentremetry was introduced by Duval-Beaupère et al., describing this method to study 3D geometry of weight forces location according to the spinopelvic skeleton, in order to

maintain a balanced and economical posture [27]. They described that the center of mass supported by hip joints was generally located in front of T9 [10]. Schwab et al. analyzed gravity line location relatively to the spine using a force plate [12]. They found that gravity line was anterior to the whole spine after 40 years, whereas it cut the L4-L5 functional unit in younger subjects. However, distance between gravity line and heels remained stable at all ages. El Fegoun et al. found significant correlation between gravity line and SVA in healthy subjects [28]. Our results also exhibited strong correlation between SVA and all COM parameters. This correlation was even stronger with ODHA (r=0.8, $p<0.001$). Among all radiographic parameters, ODHA presented the highest correlation coefficient with whole-body COM. This could imply that ODHA may be used in certain cases as an approximated surrogate parameter to estimate gravity line if barycentremetric data are not available. Further studies are required to confirm this hypothesis. However, these results are in accordance with Steffen et al.'s conclusions, highlighting strong correlation between sagittal inclination of the center of acoustic meati (CAM) to the hips center axis and CAM-gravity line [13].

PT increase was significantly associated with a posterior translation of COM at LL apex. A greater LL was associated with a more posteriorly located COM above TK apex, which underlines the importance of maintaining sufficient LL in order to keep economical alignment. Interestingly, when focusing on distal versus proximal LL, only proximal LL was associated with COM location above TK apex. To apply these results in adult spinal deformity (ASD) surgery: if too much correction is given in the upper lumbar spine, with a hyperlordotic segment, the COM above TK apex shifts posteriorly, and may explain the occurrence of proximal junctional failure (PJF), particularly in case of long fusions spanning from upper thoracic to the pelvis. Indeed, patients with posteriorly inclined fused spines would attempt to rebalance their alignment by shifting anteriorly the unfused segments on top

of the construct, increasing mechanical constraints at the proximal junction. Other authors identified dorsally displaced L1 relative to gravity line as a risk factor for PJF after ASD surgery [29]. Conversely, insufficient LL would lead to an anterior COM above TK apex, also increasing constraints on upper instrumented vertebra (UIV). Moreover, COM of the upper body is also of utmost importance in the setting of vertebral fractures. Thus, Heidsieck et al. determined a significant decrease in L1 vertebral strength with age-related alignment changes towards a more anterior COM above L1 [11].

Subjects with greater thoracic kyphosis presented more posteriorly located COM at inflexion point. Proximal and distal kyphosis did not correlate with COM, while a greater middle TK was expectedly associated with a more posterior COM at TK apex. To apply these conclusions in ASD surgery: correcting LL is important to align upper trunk segment, but restoring TK in its middle part is also fundamental to shift thoracolumbar COM backwards. Moreover, it is essential to assess thoracic kyphosis when a long fusion stopping in the lower thoracic area is planned as it regulates mechanical constraints at the thoracolumbar junction. For example, LL hypercorrection under a flat unfused thoracic spine would lead to an anterior shift of COM at inflexion point and above TK apex, and a major risk of PJF.

Several COM location parameters were used in this study at inflexion point and apexes, as they are important links in the spinal chain, from a mechanical standpoint. This study provides normative values in healthy subjects of these COM locations with respect to the vertical passing through the center of the femoral heads' axis. Their relevance varies according to the UIV choice in the setting of ASD surgery.

The "big belly effect", measured in this study through higher distance between the spine and anterior body envelope, was associated with a major anterior shift of whole-body COM and ODHA. Likely due to increased lever arm forces applied to the spine, TK increased and both distal and proximal LL decreased. As a result, compensatory mechanisms were recruited

to maintain balance, mainly through hip extension. Passias et al. exhibited significant associations between body mass index and sagittal alignment [19]. They found significantly higher SVA, PT, TPA and PI-LL mismatch in obese patients, which is in accordance with our results. Hence, variation in spinal curvatures in obese patients must be taken into account when considering extensive fusion in these patients.

Limitations

In patients with large waist line, radiographic field of view is not sufficient to include the whole-body width. In these patients, body envelope was approximated in the cut zone in coherence with the rest of body envelope. Second, there were no obese patients in this cohort, which limits the assessment of increased abdominal volume impact on alignment and COM locations in these patients. Another limitation is that the model used did not allow to contour breast precisely in female subjects to assess the impact of its volume on spinopelvic alignment parameters. Last, a greater number of subjects included in this cohort might have enabled us to highlight more significant relationships.

CONCLUSION

Barycentremetry showed that greater lumbar lordosis was associated with posterior shift of COM above thoracic apex while a greater thoracic kyphosis was correlated with a more posterior COM at inflexion point. Whole-body COM was strongly correlated with ODHA. This study also exhibited significant alignment disruption associated with increased abdominal volume, with compensatory hip extension.

These results may help understand postural alignment and compensatory mechanisms. A barycentremetric study after ASD surgery appears relevant to seek correlations between COM locations and the occurrence of mechanical complications.

REFERENCES

1. Glassman SD, Bridwell K, Dimar JR, et al. The Impact of Positive Sagittal Balance in Adult Spinal Deformity. *Spine (Phila Pa 1976)* 2005;30:2024–9.
2. Jackson RP, McManus AC. Radiographic analysis of sagittal plane alignment and balance in standing volunteers and patients with low back pain matched for age, sex, and size. A prospective controlled clinical study. *Spine (Phila Pa 1976)* 1994;19:1611–8.
3. Legaye J, Duval-Beaupère G, Hecquet J, et al. Pelvic incidence: A fundamental pelvic parameter for three-dimensional regulation of spinal sagittal curves. *Eur Spine J* 1998;7:99–103.
4. Roussouly P, Gollogly S, Berthonnaud E, et al. Classification of the normal variation in the sagittal alignment of the human lumbar spine and pelvis in the standing position. *Spine (Phila Pa 1976)* 2005;30:346–53.
5. Laouissat F, Sebaaly A, Gehrchen M, et al. Classification of normal sagittal spine alignment: refounding the Roussouly classification. *Eur Spine J* 2017;27:2002–11.
6. Ouchida J, Nakashima H, Kanemura T, et al. The age-specific normative values of standing whole-body sagittal alignment parameters in healthy adults: based on international multicenter data. *Eur Spine J* 2023;32:562–70.
7. Ouchida J, Nakashima H, Kanemura T, et al. Racial differences in whole-body sagittal alignment between Asians and Caucasians based on international multicenter data. *Eur*

Spine J. Epub ahead of print 2023. DOI: 10.1007/s00586-023-07829-8.

8. Janssen MMA, Drevelle X, Humbert L, et al. Differences in male and female spino-pelvic alignment in asymptomatic young adults: a three-dimensional analysis using upright low-dose digital biplanar X-rays. *Spine (Phila Pa 1976)* 2009;34:E826-32.
9. Sardar ZM, Cerpa M, Kelly M, et al. Age and Gender Based Spinopelvic and Regional Spinal Alignment in Asymptomatic Adult Volunteers: Results of the Multi-Ethnic Alignment Normative Study (MEANS). *Spine (Phila Pa 1976)* 2022;47:1382–90.
10. Duval-Beaupere G, Schmidt C, Cosson P. A Barycentremetic Study of the Sagittal Shape of Spine and Pelvis: The Conditions Required for an Economic Standing Position. Annals of Biomedical Engineering, Volume 20, pp 451-462, 1992. *Ann Biomed Eng* 1992;20:451–62.
11. Heidsieck C, Gajny L, Travert C, et al. Effect of postural alignment alteration with age on vertebral strength. *Osteoporos Int* 2022;33:443–51.
12. Schwab F, Lafage V, Boyce R, et al. Gravity line analysis in adult volunteers: Age-related correlation with spinal parameters, pelvic parameters, and foot position. *Spine (Phila Pa 1976)* 2006;31:959–67.
13. Steffen JS, Obeid I, Aurouer N, et al. 3D postural balance with regard to gravity line: An evaluation in the transversal plane on 93 patients and 23 asymptomatic volunteers. *Eur Spine J* 2010;19:760–7.
14. Dubousset J. Three-dimensional analysis of the scoliotic deformity. In: Weinstein L, ed. *The Pediatric Spine: Principles and Practice*. 1994.
15. Hernandez T, Thenard T, Vergari C, et al. Coronal trunk imbalance in idiopathic scoliosis: Does gravity line localisation confirm the physical findings? *Orthop Traumatol Surg Res* 2018;104:617–22.
16. Nérot A, Choisne J, Amabile C, et al. A 3D reconstruction method of the body

envelope from biplanar X-rays: Evaluation of its accuracy and reliability. *J Biomech* 2015;48:4322–6.

17. Amabile C, Choisne J, Nérot A, et al. Determination of a new uniform thorax density representative of the living population from 3D external body shape modeling. *J Biomech* 2016;49:1162–9.
18. Dempster WT. Geometrical, Kinematic, and Mechanical Aspects of the body with special reference to the limbs. 1995;1–254.
19. Passias PG, Segreto FA, Imbo B, et al. Defining age-adjusted spinopelvic alignment thresholds: should we integrate BMI? *Spine Deform* 2022;10:1077–84.
20. Chaibi Y, Cresson T, Aubert B, et al. Fast 3D reconstruction of the lower limb using a parametric model and statistical inferences and clinical measurements calculation from biplanar X-rays. *Comput Methods Biomech Biomed Engin* 2012;15:457–66.
21. Humbert L, De Guise JA, Aubert B, et al. 3D reconstruction of the spine from biplanar X-rays using parametric models based on transversal and longitudinal inferences. *Med Eng Phys* 2009;31:681–7.
22. Amabile C, Pillet H, Lafage V, et al. A new quasi-invariant parameter characterizing the postural alignment of young asymptomatic adults. *Eur Spine J* 2016;25:3666–74.
23. Lafage R, Steinberger J, Pesenti S, et al. Understanding Thoracic Spine Morphology, Shape, and Proportionality. *Spine (Phila Pa 1976)* 2020;45:149–57.
24. Pesenti S, Charles YP, Prost S, et al. Spinal Sagittal Alignment Changes During Childhood. *J Bone Jt Surg* 2023;105:676–86.
25. Charles YP, Prost S, Pesenti S, et al. Variation of cervical sagittal alignment parameters according to gender, pelvic incidence and age. *Eur Spine J* 2022;31:1228–40.
26. Passias PG, Jalai CM, Diebo BG, et al. Full-Body Radiographic Analysis of

Postoperative Deviations From Age-Adjusted Alignment Goals in Adult Spinal Deformity Correction and Related Compensatory Recruitment. *Int J spine Surg* 2019;13:205–14.

27. Duval-Beaupère G, Robain G. Visualization on full spine radiographs of the anatomical connections of the centres of the segmental body mass supported by each vertebra and measured in vivo. *Int Orthop* 1987;11:261–9.

28. El Fegoun AB, Schwab F, Gamez L, et al. Center of gravity and radiographic posture analysis: A preliminary review of adult volunteers and adult patients affected by scoliosis. *Spine (Phila Pa 1976)* 2005;30:1535–40.

29. Xi Z, Duan P-G, Mummaneni P V, et al. Posterior Displacement of L1 May be a Risk Factor for Proximal Junctional Kyphosis After Adult Spinal Deformity Correction. *Glob spine J* 2023;13:1042–8.

Figure 1: Representation of successive steps for skeletal and body envelope 3D reconstruction, in sagittal view. A: raw EOS® image. B: identification of bony structures and joints, and body envelope points. C: adjustment of generated model to fit bony contours (in red) and body envelope contours (in green). D: 3D visualization of body envelope.

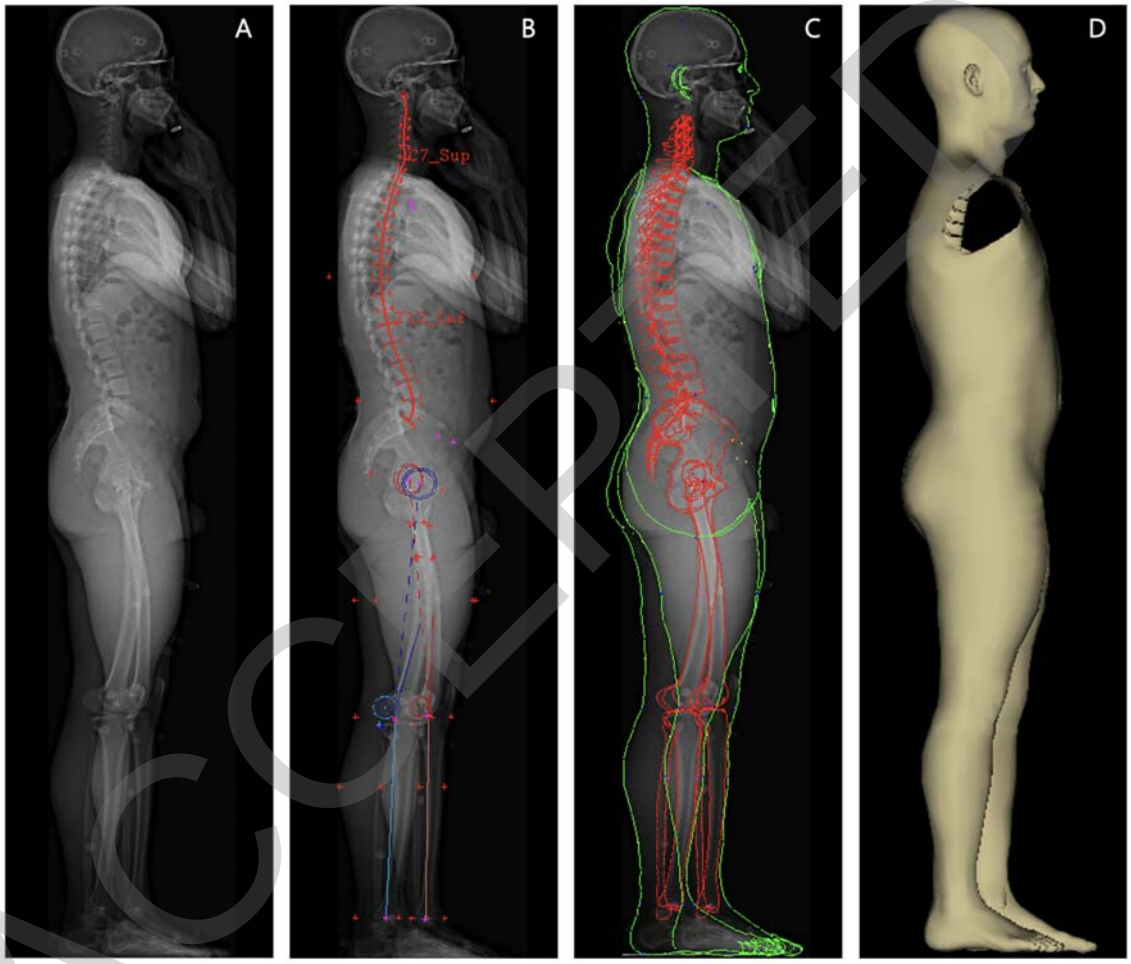

Figure 2: 3D reconstruction of the skeleton from C3 to the tibias and body envelope. The three red segments represent the distances between anterior skin and vertebral body center at lumbar lordosis apex, at inflexion point and thoracic kyphosis apex. The body segment above lumbar lordosis apex is colored in green. Its center of mass is represented by the green star. The center of the femoral head axis is the 3D plane origin.

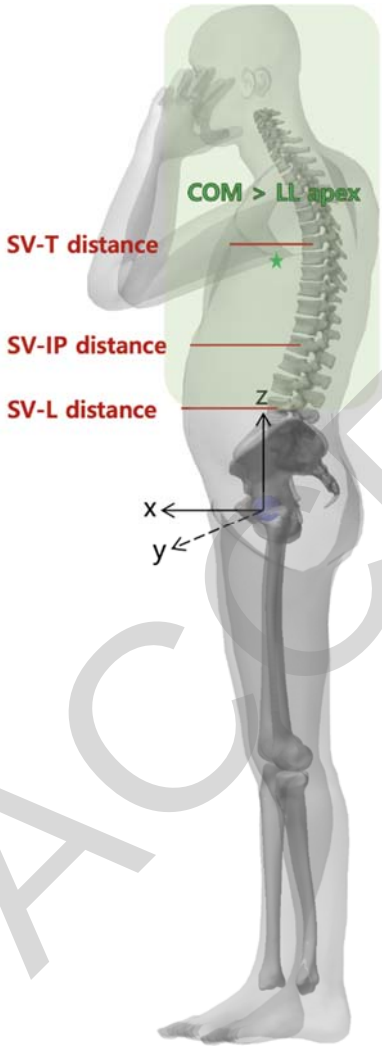

Figure 3: Illustration of the whole-body segmentation after body envelope reconstruction.

Figure 4: Representation of correlations between spinal curvatures and COM locations. A greater lumbar lordosis was associated with more posterior COM above TK apex (through proximal LL increase). Greater thoracic kyphosis was correlated with more posterior COM at inflexion point.

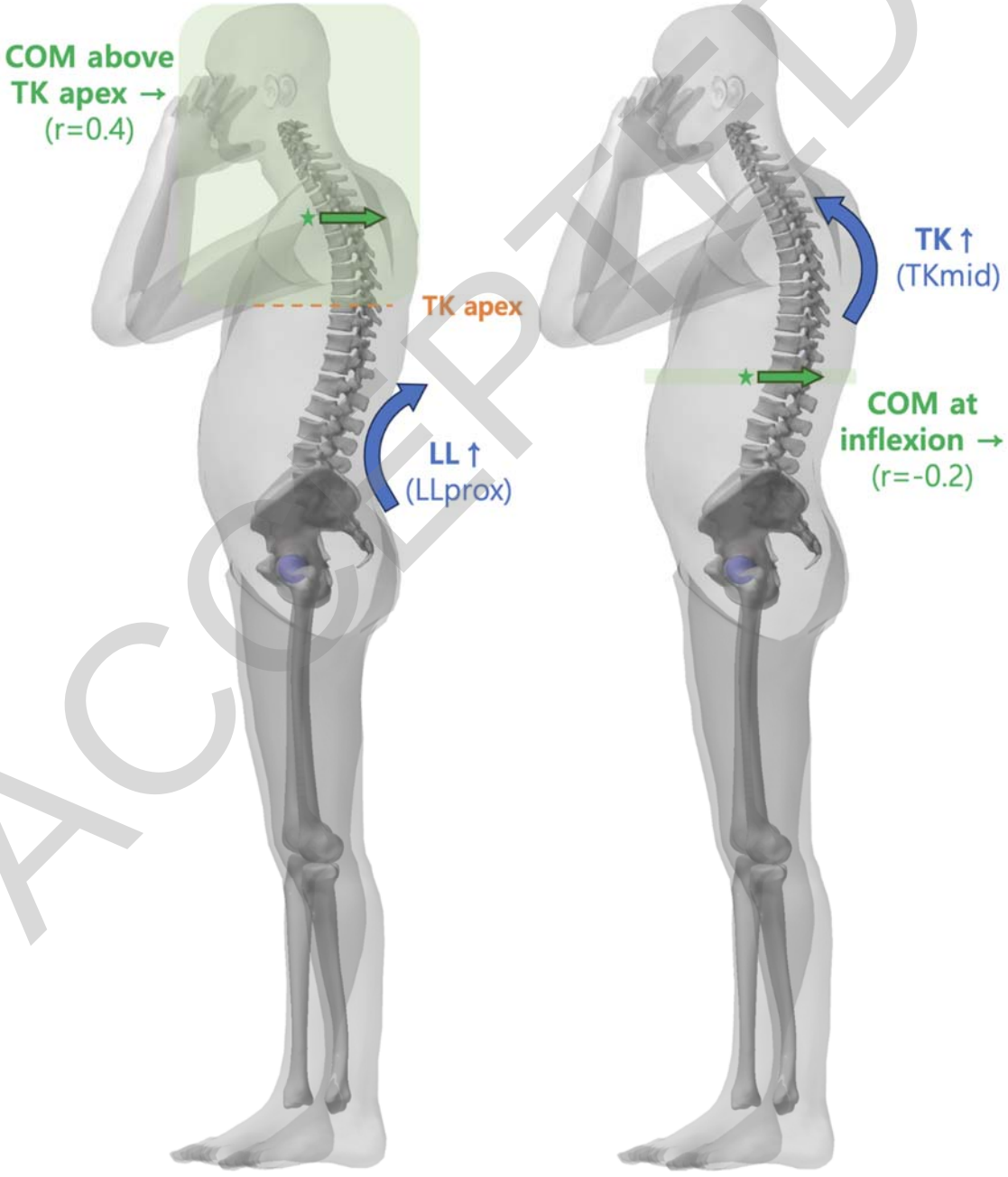

Figure 5: Plot representations of COM above TK apex, above LL apex, above inflexion point and whole-body COM according to ODHA.

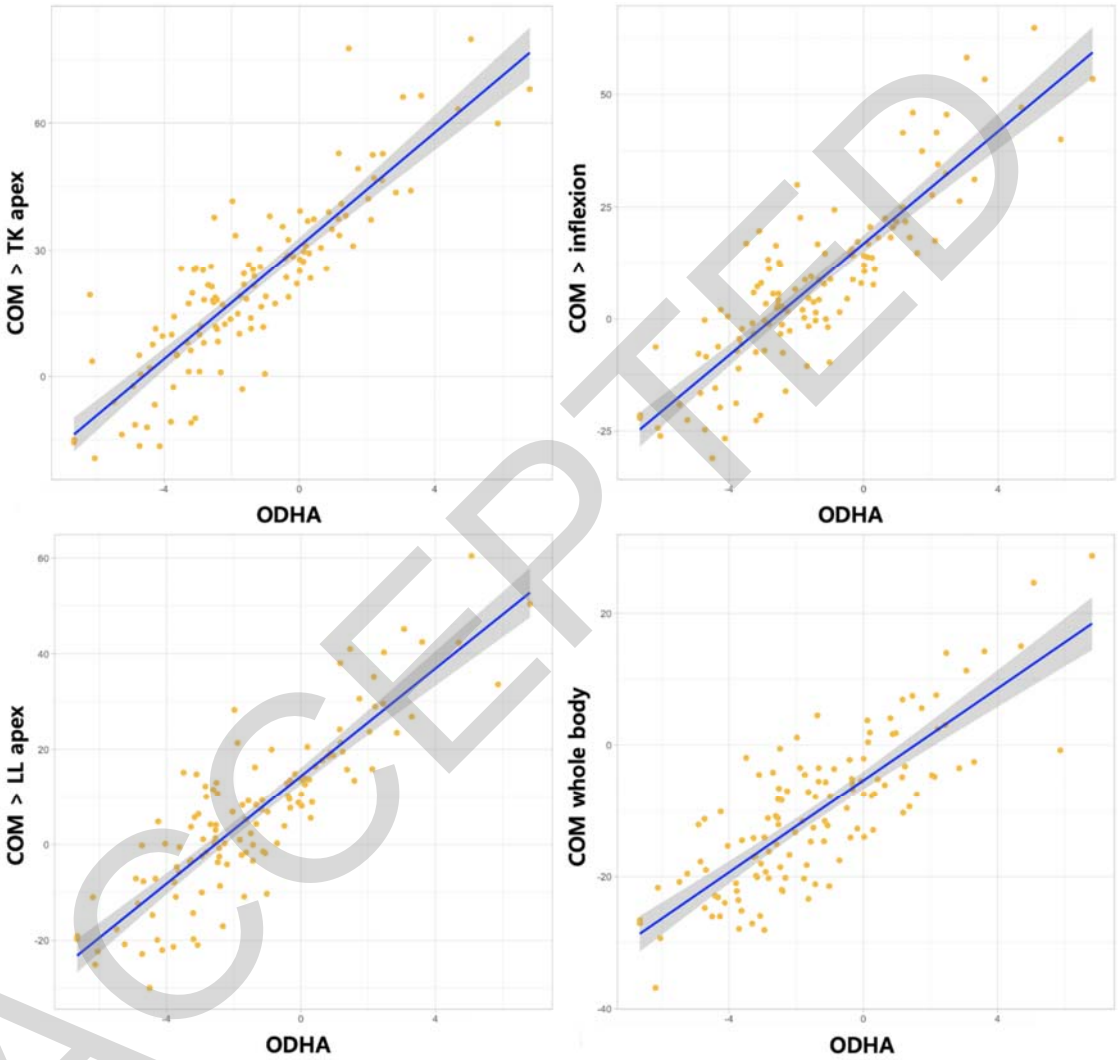

Figure 6: Illustration of the "big belly effect". Increased SV-L distance was associated with decreased LLprox and LLdist, increased TK leading to more anterior body COM and ODHA. A greater hip extension was recruited to compensate for this malalignment.

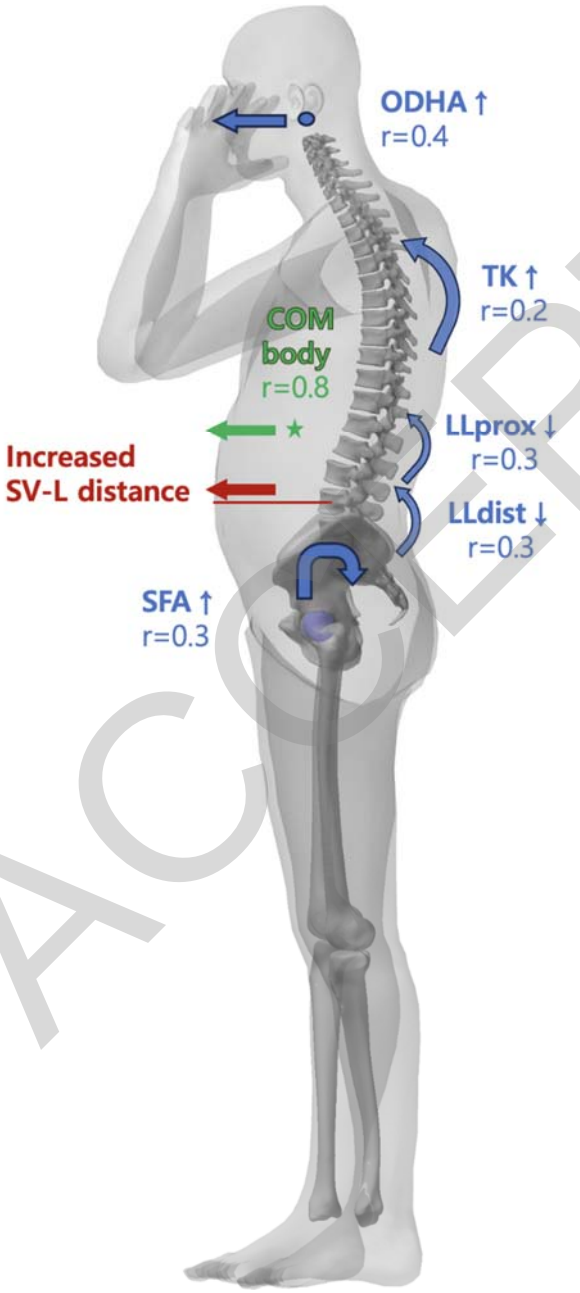

Table 1: Demographic, radiographic and barycentremetric parameters description in the cohort. *SD = Standard deviation. COM > LL apex = COM above LL apex*

n=124	**Mean**	**Median**	**SD**	**Min**	**Max**	**Shapiro**
Age	43.8	40.0	19.3	20	88	*<0.001*
Weight	69.4	69.5	11.8	45	93	*0.02*
Height	171.4	172.0	8.4	153	188	*0.15*
BMI	23.4	23.3	2.9	16.7	29.8	*0.15*
Radiographic parameters						
PI	49.4	49.1	9.7	30.8	72.6	*0.06*
SS	37.3	36.9	8.3	14.2	60.8	*0.98*
PT	12.1	12.6	7.1	-3.9	27.9	*0.61*
LL	-62.5	-61.7	13.7	-97.1	-23.9	*0.87*
LLprox	-19.1	-19.8	9.0	-39.7	8.7	*0.71*
LLdist	-43.4	-43.3	10.1	-69.5	-11.6	*0.66*
TK	54.8	54.8	12.2	26.3	86.8	*0.68*
TKprox	20.0	19.6	8.7	-4.4	59.7	*0.001*
TKmid	23.8	23.8	7.5	8.8	45.8	*0.33*
TKdist	6.9	6.7	7.6	-11.4	37.7	*0.08*
CL	-6.8	-6.7	11.0	-41.9	19.4	*0.94*
CLprox	-3.3	-2.7	9.6	-24.7	19.4	*0.49*
CLdist	-3.5	-3.2	6.9	-19.4	13.7	*0.66*
SSA	129.4	129.0	9.6	100.2	153.3	*0.51*
TPA	7.2	6.7	7.2	-10.9	23.9	*0.66*
SVA	-3.2	-3.3	26.7	-58.4	73.3	*0.16*
ODHA	-1.4	-1.7	2.6	-6.7	6.8	*0.05*
PSh	18.7	5.1	32.9	-35.6	93.9	*<0.001*
SFA	196.4	196.9	7.7	178.4	211.4	*0.16*
KFA	4.9	4.2	3.2	0.5	16.9	*<0.001*
AFA	-2.7	-2.4	2.9	-12.9	5.6	*0.31*
Barycentric parameters						
COM body	-10.4	-11.1	11.4	-36.8	28.7	*0.02*
COM > LL apex	6.3	5.6	17.2	-29.9	60.5	*0.07*
COM > Inflexion	7.9	6.9	19.0	-19.4	79.8	*0.02*
COM > TK apex	21.3	20.5	20.3	-31.1	64.8	*0.08*
COM at LL apex	2.8	1.7	11.7	-28.7	46.9	*0.15*
COM at inflexion	-12.3	-12.8	15.3	-58.1	28.7	*0.86*
COM at TK apex	-46.1	-48.6	25.3	-97.0	77.1	*<0.001*
SV-L distance	137.2	130.9	35.3	63.5	212.9	*0.006*
SV-IP distance	146.8	142.5	32.8	80.6	223.7	*0.02*
SV-T distance	145.4	141.8	27.0	74.4	226.2	*0.43*

Table 2: Correlation table of barycentremetric parameters with body mass index and age.

Significant correlations arre written in bold. *COM > LL apex = COM above LL apex*

Correlations	BMI		Age	
	r	*p*	r	*p*
COM body	**0.3**	***0.004***	**0.3**	***0.006***
COM > LL apex	**0.3**	***0.004***	0.2	*0.05*
COM > inflexion	**0.3**	***0.003***	0.2	*0.06*
COM > TK apex	**0.3**	***<0.001***	0.2	*0.06*
COM at LL apex	**0.3**	***0.009***	**0.2**	***0.04***
COM at inflexion	**0.3**	***0.005***	**0.3**	***0.005***
COM at TK apex	0.2	*0.05*	0.2	*0.05*
SV-L distance	**0.7**	***<0.001***	**0.7**	***<0.001***
SV-IP distance	**0.8**	***<0.001***	**0.6**	***<0.001***
SV-T distance	**0.6**	***<0.001***	**0.6**	***<0.001***

Table 3: Correlation table. All significant correlations are written in bold. Correlation coefficient are marked with a "*" if p-values<0.05, and with "†" if p-value<0.001.

Correlations	PT	LL	TK	CL	SFA	ODHA
COM body	-0.1	**0.3 ***	0.1	-0.1	**-0.3 ***	**0.8 †**
COM > LL apex	-0.2	**0.3 ***	-0.1	0.1	**-0.3 ***	**0.9 †**
COM > inflexion	-0.1	**0.3 ***	0	0.1	**-0.2 ***	**0.8 †**
COM > TK apex	-0.1	**0.3 †**	-0.1	0.1	**-0.2 ***	**0.9 †**
COM at LL apex	**-0.3 †**	0.1	0	0	**-0.4 †**	**0.5 †**
COM at inflexion	-0.1	**0.2 ***	**-0.2 ***	0.1	**-0.1**	**0.6 †**
COM at TK apex	-0.1	0.1	0	0	**-0.2**	**0.7 †**
SV-L distance	**0.4 †**	**0.4 †**	**0.2 ***	**-0.3 †**	**0.3 †**	**0.4 †**
SV-IP distance	**0.3 †**	**0.4 †**	**0.2 ***	**-0.3 ***	**0.2 ***	**0.4 †**
SV-T distance	**0.2 ***	0.2	**0.5 †**	**-0.4 †**	**0.3**	**0.3 †**
BMI	**0.2 ***	**0.3 ***	0.1	**-0.2 ***	0.1	**0.3 ***
Age	**0.5 †**	**0.4 †**	**0.3 ***	**-0.3 †**	**0.4 †**	**0.3 †**
PI	**0.6 †**	**-0.5 †**	0	0	**0.5 †**	-0.1
SS	**-0.2 ***	**-0.8 †**	-0.1	**0.2 ***	-0.2	-0.2
PT	-	**0.2 ***	0.1	**-0.2 ***	**0.9 †**	0
LL	**0.3 ***	-	**-0.3 ***	0	0.2	**0.4 †**
LL prox	0	-	**-0.3 ***	0	0	**0.3 †**
LL dist	**0.3 †**	-	0	0	**0.2 ***	**0.3 ***
TK	0.1	**-0.2 ***	-	**-0.7 †**	0	0.1
TK prox	0.2	**0.2 ***	-	**-0.4 †**	0.1	0.2
TK mid	0.1	**-0.3 ***	-	**-0.4 †**	0.1	0
TK dist	-0.1	**-0.3 †**	-	**-0.3 †**	-0.1	-0.1
CL	**-0.2 ***	0	**-0.7 †**	-	-0.1	0
CL prox	**-0.2 ***	0	**-0.5 †**	-	-0.2	-0.2
CL dist	0	0.1	**-0.5 †**	-	0	0.1
SSA	**-0.3 †**	**-0.9 †**	-0.1	**0.3 ***	**-0.3 ***	**-0.4 †**
TPA	**0.9 †**	**0.4 †**	0.1	**-0.2 ***	**0.8 †**	**0.3 †**
SVA	**0.4 †**	**0.5 †**	0.1	**-0.3 ***	**0.3 ***	**0.8 †**
ODHA	0	**0.4 †**	0.1	0	-0.1 *	-
PSh	0	0.1	0	**0.2 ***	0	**0.3 ***
SFA	**0.9 †**	0.2	0	-0.1	-	-0.1
KFA	0.1	0	0	0	0.2	-0.1
AFA	**-0.1 ***	-0.1	-0.1	0.1	**0.2 ***	-0.1

Table 4: Description of ß coefficients and intercepts from multiple linear regressions. The five regression models are represented in separate columns. Coefficients are marked with a "*" if p-values<0.05, and with "†" if p-value<0.001. *COM > LL apex = COM above LL apex*

ß	**PT**	**LL**	**TK**	**CL**	**SFA**
Intercept	88.8 †	-7.47	14.5 *	-9.1	217.9 †
BMI	-0.01	0.64*	-	-0.23	-
Age	0	0.02	0.11 *	-0.04	0
COM body	-	0.24 *	-	-	-0.48 †
COM at LL apex	-0.01 *	-	-	-	0.11 †
COM at inflexion	-	-0.06	-0.13 *	-	-
COM at TK apex	-	-	-	-	-
COM > LL apex	-	0.06	-	-	0.20
COM > inflexion	-	-0.35	-	-	-0.03
COM > TK apex	-	0.25 *	-	-	-0.01
SV-L distance	0.01 †	-0.03	-0.08	-0.06	0
SV-IP distance	0	-0.04	0.04	-0.01	0
SV-T distance	-0.01 *	-	0.14 *	0.14 *	-
PI	0.96 †	0.04	-	-	0.38
PT	-	-	-	2.81	0.78
SS	-	-1.29 †	-	-	-
LL	-0.01	-	-0.10	-	-
LLdist	0.01*	-	-	-	-0.03
LLprox	-	-	-0.35 †	-	-
TK	-	-0.31 †	-	-0.73 †	-
CLdist	0	-	-0.70 †	-	-
CLprox	0	-	-0.51 †	-	-
TPA	0.02	-	-	-3.42	-0.17
SVA	-0.12 †	0.10	-	0.26	-0.02
SSA	-0.97 †	-	-	0.22	-0.42
SFA	0.01	-	-	-	-
PSh	-	-	-	0.06 *	-
AFA	-0.01	-	-		0.44 †
Performance metrics					
Standard error	0.24	4.94	6.95	7.23	1.37
Adjusted R^2	0.999	0.86	0.67	0.58	0.97

Table 5: Association between increased SV-L distance with univariate correlations, and ß coefficients resulting from stepwise multivariate linear regression, including only significantly associated parameters in univariate analysis. Respective p-values are reported, and written in bold if significant.

Increased ***SV-L distance***	***r***	***univariate p***	***ß coeff.***	***multivariate p***
COM body	**0.8**	*<0.001*	**2.52**	*<0.001*
ODHA	**0.4**	*<0.001*	**-4.65**	*0.005*
CLprox	**-0.4**	*<0.001*	-0.32	*0.23*
TK	**0.2**	*0.003*	**0.82**	*<0.001*
LLprox	**0.3**	*<0.001*	**1.49**	*<0.001*
LLdist	**0.3**	*<0.001*	**0.49**	*0.04*
PT	**0.4**	*<0.001*	-0.91	*0.30*
SFA	**0.3**	*<0.001*	**2.98**	*<0.001*

Regression model metrics: R^2: 0.53, standard error= 23.3